To be published in SPIE Proc. Vol. 8160-33, SPIE Optical Engineering + Applications, San Diego, Aug 21-25, 2011

Full Stokes polarization camera

M. Vedel*[a], S. Breugnot[a], N. Lechocinski[a]
[a]Bossa Nova Technologies, 606 Venice Blvd Suite B, Venice, CA, USA 90291

ABSTRACT

Objective and background: We present a new version of Bossa Nova Technologies' passive polarization imaging camera. The previous version was performing live measurement of the Linear Stokes parameters (S_0, S_1, S_2), and its derivatives. This new version presented in this paper performs live measurement of Full Stokes parameters, i.e. including the fourth parameter S_3 related to the amount of circular polarization. Dedicated software was developed to provide live images of any Stokes related parameters such as the Degree Of Linear Polarization (DOLP), the Degree Of Circular Polarization (DOCP), the Angle Of Polarization (AOP).

Results: We first we give a brief description of the camera and its technology. It is a Division Of Time Polarimeter using a custom ferroelectric liquid crystal cell. A description of the method used to calculate Data Reduction Matrix (DRM)[5,9] linking intensity measurements and the Stokes parameters is given. The calibration was developed in order to maximize the condition number of the DRM. It also allows very efficient post processing of the images acquired. Complete evaluation of the precision of standard polarization parameters is described. We further present the standard features of the dedicated software that was developed to operate the camera. It provides live images of the Stokes vector components and the usual associated parameters. Finally some tests already conducted are presented. It includes indoor laboratory and outdoor measurements. This new camera will be a useful tool for many applications such as biomedical, remote sensing, metrology, material studies, and others.

Keywords: Time division polarimeter, polarization imaging, Stokes parameters, visible band, retardance mapping, target detection/identification, 3D reconstruction,

1 INTRODUCTION

Along with the intensity and the spectrum, the polarization of light carries abundant information[1-8]. Polarization is by far the less investigated of these three fundamental properties of the light. Various technological approaches of imaging polarimeters have been studied[9-17]. We present in this paper the technology, its calibration method and some experimental results of the new version of Bossa Nova Technologies' full Stokes imaging polarimeter. This camera performs live measurement of the four Stokes parameters of a scene. This Polarization State Analyzer (PSA) is a Division of Time Polarimeter[9] based on two ferroelectric liquid crystal cells and a linear polarizer.

We will first detail the technology of the imaging polarimeter (Section 3). We will then describe the calibration process based on Data Reduction Matrix method (Section 4). In Section 5 we will comment some experimental results conducted in order to evaluate the camera's performances. Finally, we will present in section 6 some polarization images acquired using dedicated software.

2 POLARIZATION IMAGING

Polarization imaging consists in measuring at least two Stokes parameters. Polarization data contained in the Stokes parameters give much more information than a simple intensity measurement. Most of the available polarization imaging cameras perform linear Stokes polarization imaging. In most cases, almost all the polarization information is contained in the three first Stokes parameters. We previously presented a Linear Stokes imaging polarimeter[17]. Circular polarization requires specific conditions to be created (light going through a birefringent medium, light reflected by a multilayer material). Therefore the last Stokes parameter contains mostly noise. However, research labs and industries have shown a growing interest for circular polarization measurements. For example, biomedical applications as well as mechanical stress measurements require to be able to quantify precisely circular polarization. Many laboratory full

Stokes imagers have been presented in the past[9,18]. The challenge is to design and manufacture such an imaging polarimeter in a compact version, with off-the-shelf optical components and electronics.

3 DIVISION OF TIME POLARIMETER

The first polarization imaging systems were division-of-time polarimeters with mechanical rotation of polarizer(s) and waveplate(s) between each frame. These systems are usually quite slow and very sensitive to motion of the scene between frames. The use of electrically driven polarization elements like ferroelectric liquid crystals (FLC) or birefringent ceramics reduced dramatically the time required to acquire the polarization frames, allowing fast division of time polarimeters to be designed, and therefore limiting the registration problem caused by the motion of the scene. We developed a fast polarization modulator composed of two elements for the first version of our camera[17]. In order to measure the full Stokes vector we had to modify the structure and the orientation of the various elements. The first element is a programmable (FLC) wave plate with a retardance close to λ/2. The second element is a programmable FLC wave plate with a retardance close to λ/4. The last element is a fixed linear polarizer. This architecture allows fast acquisition of four polarization frames that are later used to calculate the Stokes vector for each pixel of the image. The critical point is to link the raw frames to the Stokes parameters. We used the data reduction method to determine the calibration matrix that permits to calculate the four Stokes parameters, given a 4-frames raw vector. The calibration process is described in the following section.

4 CALIBRATION

4.1 Mathematical model

Calibrating the camera consists in experimentally determining the Data Reduction Matrix[3] parameters. We used the method developed The DRM links the 4 measured intensities (one for each position of the PSA) to any unknown incident Stokes vector.

$$\mathbf{X} = \begin{bmatrix} \boldsymbol{I_{raw1}} \\ \boldsymbol{I_{raw2}} \\ \boldsymbol{I_{raw3}} \\ \boldsymbol{I_{raw4}} \end{bmatrix} = \mathbf{C} \cdot \boldsymbol{S_{in}} \tag{1}$$

Where C is the PSA matrix, its inverse is the DRM.

Each state **i** of the PSA has its own Mueller matrix. For any incident Stokes vector the measured polarization state would be:

$$\boldsymbol{S_{out}^{state\ i}} = \begin{bmatrix} \boldsymbol{S_{0,out}^{i}} \\ \boldsymbol{S_{1,out}^{i}} \\ \boldsymbol{S_{2,out}^{i}} \\ \boldsymbol{S_{3,out}^{i}} \end{bmatrix} = \begin{bmatrix} \boldsymbol{m_{00}^{state\ i}} & \boldsymbol{m_{01}^{state\ i}} & \boldsymbol{m_{02}^{state\ i}} & \boldsymbol{m_{03}^{state\ i}} \\ \boldsymbol{m_{10}^{state\ i}} & \boldsymbol{m_{11}^{state\ i}} & \boldsymbol{m_{12}^{state\ i}} & \boldsymbol{m_{13}^{state\ i}} \\ \boldsymbol{m_{20}^{state\ i}} & \boldsymbol{m_{21}^{state\ i}} & \boldsymbol{m_{22}^{state\ i}} & \boldsymbol{m_{23}^{state\ i}} \\ \boldsymbol{m_{30}^{state\ i}} & \boldsymbol{m_{31}^{state\ i}} & \boldsymbol{m_{32}^{state\ i}} & \boldsymbol{m_{33}^{state\ i}} \end{bmatrix} \cdot \boldsymbol{S_{in}} \tag{2}$$

The sensor used is not sensitive to polarization. Therefore only the first row of the Mueller matrix is useful. Thus, each intensity measured will be written as in Equation 3:

$$\boldsymbol{S_{0,out}^{PSAi}} = \boldsymbol{m_{00}^{i}} . \boldsymbol{S_{0,in}} + \boldsymbol{m_{01}^{i}} . \boldsymbol{S_{1,in}} + \boldsymbol{m_{02}^{i}} . \boldsymbol{S_{2,in}} + \boldsymbol{m_{03}^{i}} . \boldsymbol{S_{3,in}} \tag{3}$$

The $\boldsymbol{m_{kl}^{i}}$ parameters need to be calculated for the four position of the PSA. Eq. 3 is a linear equation with four unknown parameters. The calibration consists in generating N>4 incident Stokes parameters and measuring $\boldsymbol{S_{0,out}^{i}}$. For the **i**th position of the PSA the resulting linear equation system can be written in a matrix form:

$$\begin{bmatrix} S_{0,out}^{0} \\ S_{0,out}^{1} \\ \vdots \\ S_{0,out}^{N} \end{bmatrix}_{i} = [(S_{in})^{T}] \cdot \begin{bmatrix} m_{00}^{i} \\ m_{01}^{i} \\ m_{02}^{i} \\ m_{03}^{i} \end{bmatrix} = \begin{bmatrix} S_{0,in}^{0} & S_{1,in}^{0} & S_{2,in}^{0} & S_{3,in}^{0} \\ S_{0,in}^{1} & S_{1,in}^{1} & S_{2,in}^{1} & S_{3,in}^{1} \\ \vdots & \vdots & \vdots & \vdots \\ S_{0,in}^{N} & S_{1,in}^{N} & S_{2,in}^{N} & S_{3,in}^{N} \end{bmatrix} . \begin{bmatrix} m_{00}^{i} \\ m_{01}^{i} \\ m_{02}^{i} \\ m_{03}^{i} \end{bmatrix} \quad \textbf{(4)}$$

where T represents the transposition. $[(\boldsymbol{S_{in}})^{T}]$ is a N × 4 matrix representing the incident known Stokes vectors. These polarization states were generated by a PSG composed of a quarter wave plate and a linear polarizer. Section 4.2 will detail the experimental setup.

The first row of the Mueller matrix corresponding to the **i**th state of the PSA can be numerically calculated. It is a linear inverse problem that can be solved using Moore-Penrose pseudo-inverse $\mathbf{A}^{+}$.

$$\begin{bmatrix} m_{00}^{state\ i} \\ m_{01}^{state\ i} \\ m_{02}^{state\ i} \\ m_{03}^{state\ i} \end{bmatrix} = [(S_{in})^{T}]^{+} \cdot \begin{bmatrix} S_{0,out}^{0} \\ S_{0,out}^{1} \\ \vdots \\ S_{0,out}^{N} \end{bmatrix} \quad \textbf{(5)}$$

This calculation is performed for each state of the PSA. We obtain the expression of the PSA matrix **C**:

$$\mathbf{X} = \begin{bmatrix} I_{raw1} \\ I_{raw2} \\ I_{raw3} \\ I_{raw4} \end{bmatrix} = \begin{bmatrix} m_{00}^{state\ 1} & m_{01}^{state\ 1} & m_{02}^{state\ 1} & m_{03}^{state\ 1} \\ m_{00}^{state\ 2} & m_{01}^{state\ 2} & m_{02}^{state\ 2} & m_{03}^{state\ 2} \\ m_{00}^{state\ 3} & m_{01}^{state\ 3} & m_{02}^{state\ 3} & m_{03}^{state\ 3} \\ m_{00}^{state\ 4} & m_{01}^{state\ 4} & m_{02}^{state\ 4} & m_{03}^{state\ 4} \end{bmatrix} \cdot S_{in} \quad \textbf{(6)}$$

The final step is a regular inversion in order to obtain the DRM. Then any unknown incident Stokes vector can be estimated.

$$\widehat{S_{in}} = C^{-1} \cdot \begin{bmatrix} I_{raw1} \\ I_{raw2} \\ I_{raw3} \\ I_{raw4} \end{bmatrix} \quad \textbf{(6)}$$

4.2 Experimental setup

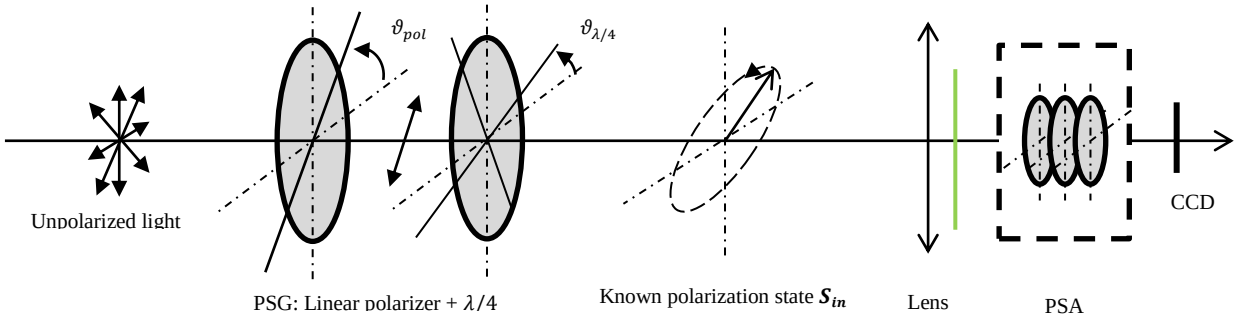

Figure 1. PSG setup for calibration

Previous work have established that in order to calculate the PSA matrix (and then the RDM), we must generate a minimum of four independent Stokes vector that form a maximum volume polyhedron inscribed inside the Poincaré sphere[9,19]. This was performed by a Polarization State Generator (PSG) composed with a high quality linear polarizer (Contrast Ratio >10,000:1) and a quarter wave plate. Both elements were mounted on a rotation stage that can be precisely controlled degree by degree (Figure 1). Therefore it was possible to generate a set of polarization states uniformly positioned on the Poincare sphere.

We also used a green filter 520/550 nm in front of the camera's objective lens. Other bandwidths are possible and give various results. However, we focused on the green bandwidth in this paper. The different RDM obtained had condition numbers ranging between 5 and 6 which insures that the inversion is reasonably well-behaved.

4.3 Calibration results

Many tests were performed to evaluate the camera's performances. We tested the camera's response with some basic incident polarization states (linear and elliptic). We computed the DOLP, AOP, DOCP and Ellipticity parameter defined by Eq. 7 and 8 and compared them to the theoretical values.

$$DOLP = \frac{\sqrt{S_1^{\,2} + S_2^{\,2}}}{S_0} \qquad AOP = \frac{1}{2} Arg(S_1 + iS_2) \tag{7}$$

$$DOCP = \frac{S_3}{S_0} \qquad \varepsilon = \frac{1}{2} Arc\sin(\frac{S_3}{S_0}) \tag{8}$$

4.4 Linear polarization

A linear polarizer with a high contrast ratio (>10,000) is rotated from 0° to 180° in front of the camera. The DOLP is expected to be 100% all the time. The AOP is supposed to follow the polarizer's axis orientation. The DOCP and the Ellipticity are expected to remain at 0% and 0° respectively.

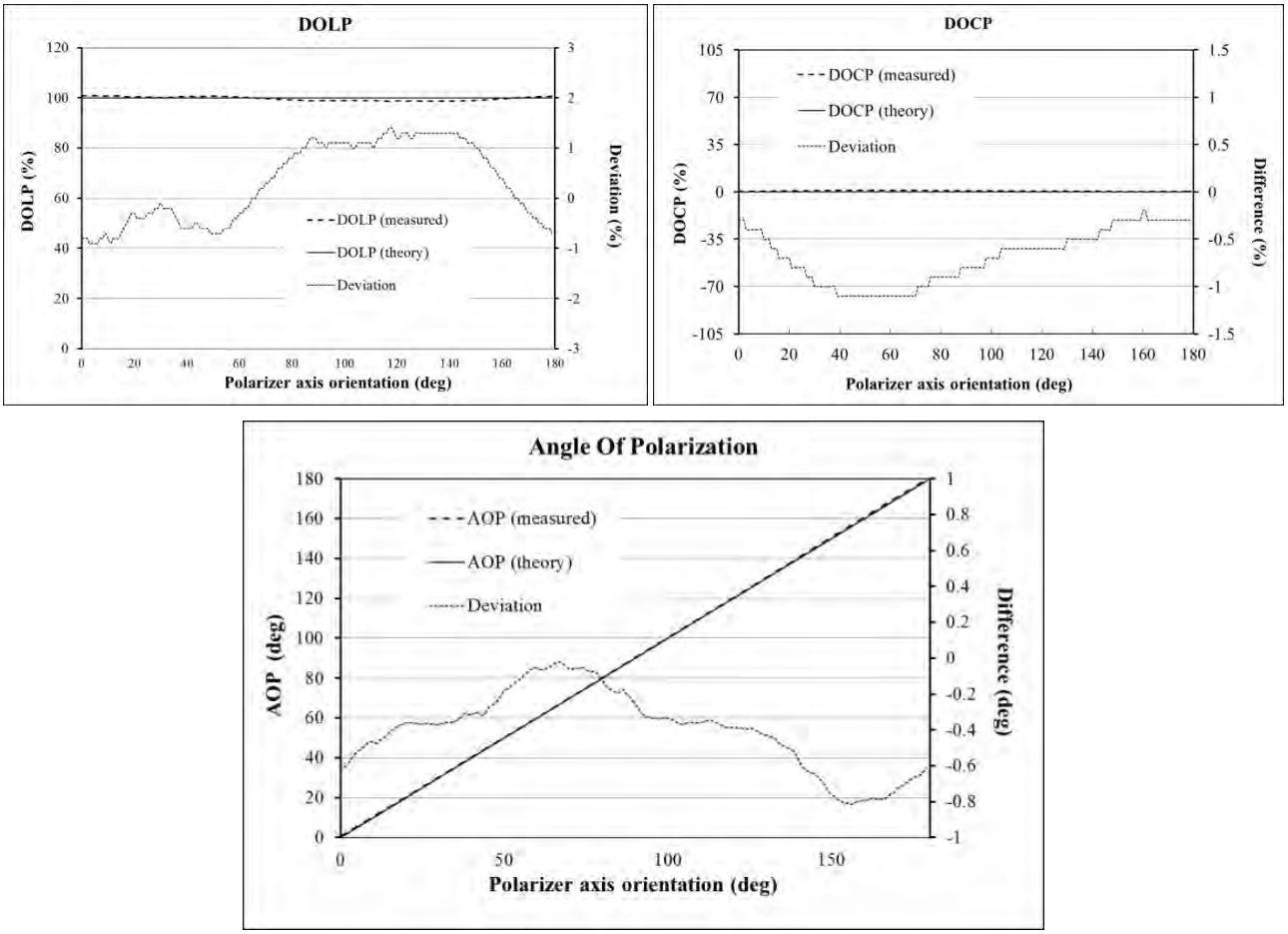

Figure 2. Measurement of the DOLP (a), DOCP(b) and AOP(c) of a rotating linear polarizer

The DOLP deviation is below 2% (peak-to-valley (P-V)) with a 0.8% standard deviation. There is a -0.5% offset error for the DOCP, repeatable (also present in the elliptic polarization test). The deviation around the mean error is below 1% (P-V), with a 0.3% standard deviation.

There is an -0.5° offset error for the AOP that is also repeatable so it can be removed. It comes from a slight difference between the polarizer reference and the PSG used for the calibration. The AOP deviation around the mean error is below 1° (P-V) and its standard deviation is below 0.22°.

4.5 Elliptic polarization ε=[-45°; 45°]; AOP = 0°

A linear polarizer with a high contrast ratio (>10,000) coupled with a quarter wave plate (QWP) are used to generate elliptic polarization states. The QWP slow axis' orientation fixes the Angle of Polarization (AOP) and the difference between the QWP slow axis orientation and the linear polarizer's axis fixes the ellipticity (-45° to 45°). In this case, the AOP remains 0° while the linear polarizer's orientation ranges from -45° to 45°.

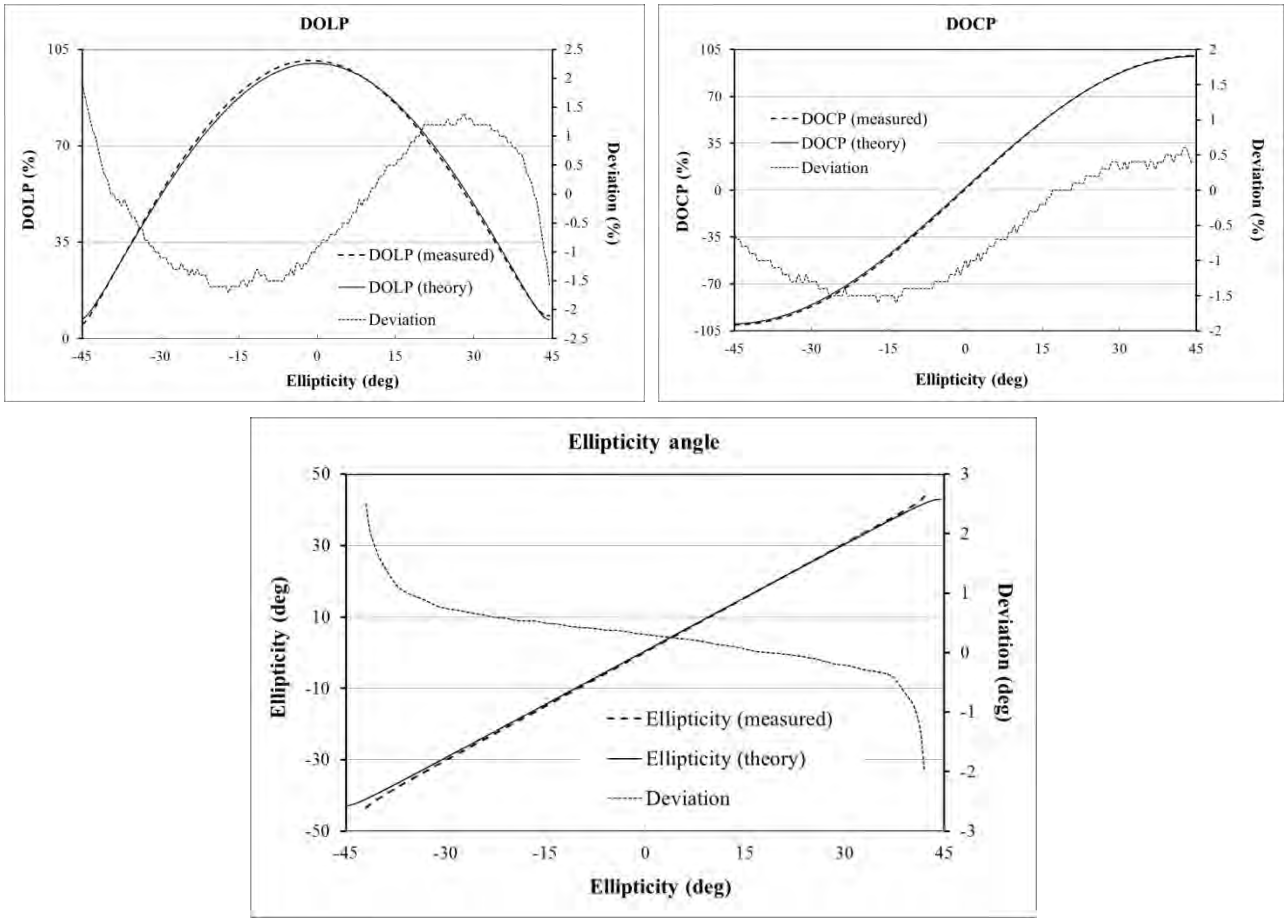

Figure 3. Measurement of the DOLP (a), DOCP(b) and AOP(c) of an elliptic polarization, ε=[-45°; 45°]

The DOLP deviation is within the same range than in the previous test. It follows the theoretical values with a 3% P-V deviation, 1% STDV. The DOCP presents the same -0.5% error offset previously measured. The DOCP deviation around the mean value remains within a 2% range (P-V), 0.75% STDV.

The ellipticity angle measured is very close to the expected values. The maximum errors are measured when close to the circular-polarization states. The deviation remains constrained within ±2° P-V, 0.6° STDV.

4.6 Summary of the results

	Linear polarization		**Elliptic polarization**	
	STDV	*P-V*	*STDV*	*P-V*
DOLP (%)	0.80%	2.00%	1.00%	3.00%
DOCP (%)	0.30%	1.00%	0.75%	2.00%
AOP (°)	0.22°	0.85°	-	-
Ellipticity (°)	0.1°	0.3°	0.6°	4°

Table 1. Results summary

The results presented herein validate the principle of the numerical calibration of the DRM. The DOLP deviation remains within ±1.5% P-V for both linear or elliptic incident polarizations. The DOCP is better with a maximum ±1% P-V deviation. Tests with different incident polarization states were performed and produced similar results.

We also calibrated the PSA for other wavelengths: 395/480nm (Blue) and >600nm (Red). The FLCs used in the PSA have a different retardance depending on the bandwidth. Therefore the RDM matrices were sensibly different, as their condition numbers were. With the Blue bandwidth we obtained CN between 2 and 3, which was better than the green bandwidth. On the other hand, the calibration in the red band provided a CN around 12, which makes the Stokes vector estimation more sensitive to any source of noise. Similar tests as those presented in the previous section were conducted with the other bandwidths. Results were shown to be in the same range.

5 FULL STOKES POLARIZATION CAMERA

A first version of this camera based on this technology has been released. The camera (Figure 4) is a Full Stokes division of time imaging polarimeter. It uses standard CCD sensor, standard C-mount lenses, and the fast polarization modulator described above. The camera standard resolution is 1M pixels with a 12-bit depth. The sensor goes up to 40 frames per seconds (fps) in full resolution, resulting in a frame rate of up to 10 fps for the calculated images. The camera is compact (80x80x100mm) and robust. The acquisition and image processing software run on a standard computer. The interface between the camera and the computer is GigE connection (fast Ethernet) and USB. The camera presented is integrated and calibrated with a green filter (520-550nm). Dedicated software was developed in order to operate the camera and perform live polarization imaging. We can now visualize in live any Stokes parameter, or their derivate (DOLP, DOCP, AOP Ellipticity, etc.). It is also convenient to add a false color coding to enhance the visualization. Some examples are given below with various objects.

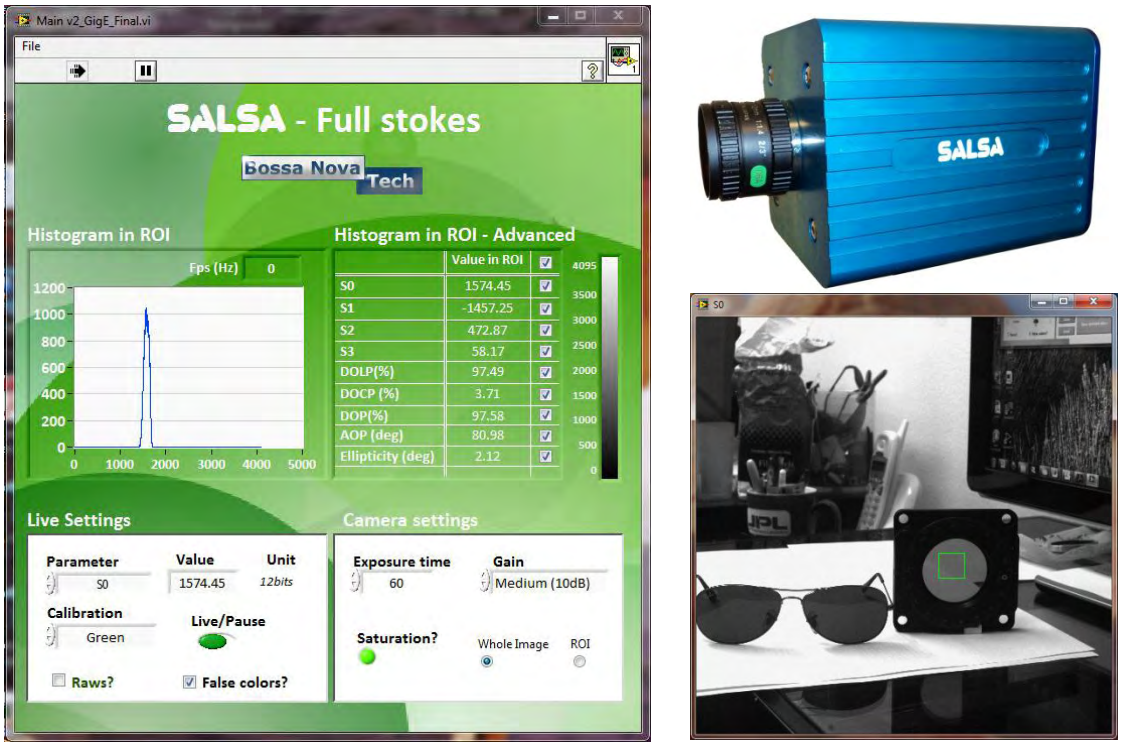

Figure 4. (a) Software front panel (b) Picture of the camera (c) S_0 live image

5.1 Stokes parameters

When the camera is calibrated, we can process the Stokes parameters to display and measure in live relevant polarization parameters. Examples will be given below on a measurement. The scene observed is made of a pair of polarized sunglasses, a linear polarizer, and monitor on the background. These objects are laid on a glass table. From the raw images acquired and the calibration matrix, the four Stokes parameters can be deduced (Figure 5).

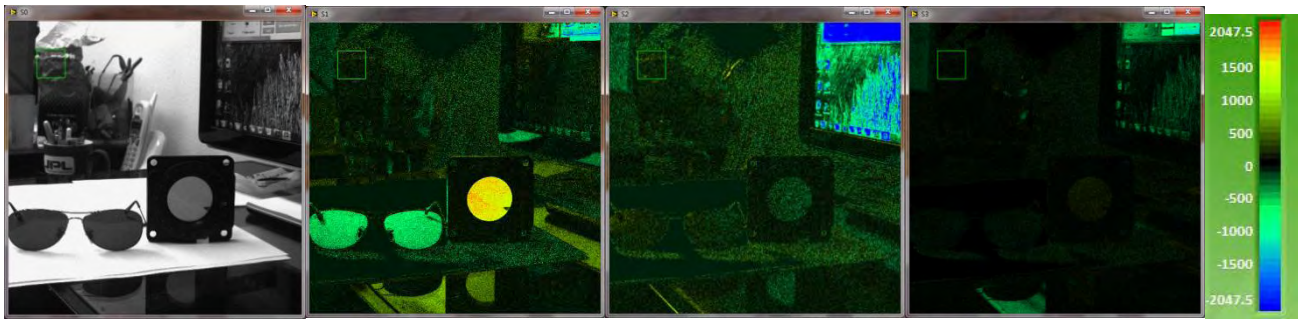

Figure 5. (a) S_0 (b) S_1 (c) S_2 (d) S_3 (e) Color bar

The Stokes parameters images are displayed using a color coding. Negative values appear from blue to green, null values are black and positive values progress from green to yellow to red. The Stokes images are not normalized by S_0 in this case but are directly calculated from the raw images using the calibration matrix.

The sunglasses and the linear polarizer appear bright on S_1. According to the color coding, the sunglasses are linearly polarized with a vertical axis of polarization and the linear polarizer's axis is close to a horizontal orientation. We can notice that the monitor in the background appears bright on the S_2 image, with a blue-green dominance. Again, according to the color coding, it means the monitor emits linearly polarized with a -45° axis of polarization. S_3 is almost black in this example.

5.2 DOLP and AOP

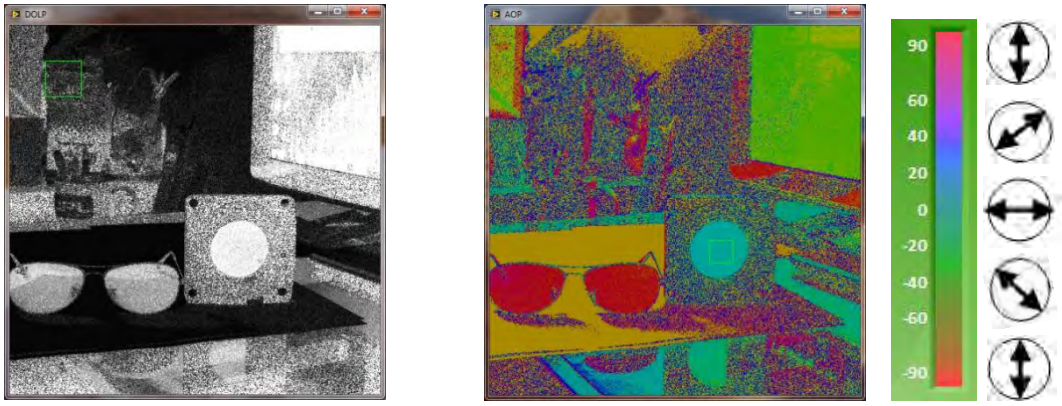

Figure 6. (a) DOLP (b) AOP as a color HUE (d) AOP color bar

Whereas all the polarization information is contained in the Stokes parameters, it can be difficult to interpret it completely. This is why more relevant parameters are computed. Figure 6a shows the DOLP image. As expected, the DOLP of the polarizer and the monitor are very high, as well as on the sunglasses. The different orientations are not distinguished. The polarizer and the glasses are laid on a white sheet of paper. The paper is white on the S_0 image because it diffuses light. In a DOLP image it appears totally black because the diffusion is non-polarized.

The best way to display the AOP is to use the color hue. Color hue is a circular scale, exactly as AOP. The hue goes from red to yellow, green, blue, magenta, and finally red again. This is exactly the case of the AOP, which can be -90°, then -45°, 0°, 45°, and finally 90° which is also -90°. Using this method there is no discontinuity between a -90° and a 90° linear polarization state.

5.3 DOCP and Ellipticity

The DOCP calculated uses the absolute value of S_3 normalized by the intensity S_0. Therefore, what is coded is the total amount of circular polarization regardless of the sign of S_3. Figure 7 shows an image of two pairs of glasses. The left pair is the same as the one used before (linearly polarized). The glasses on the right are commonly used in many 3D movie theatres.

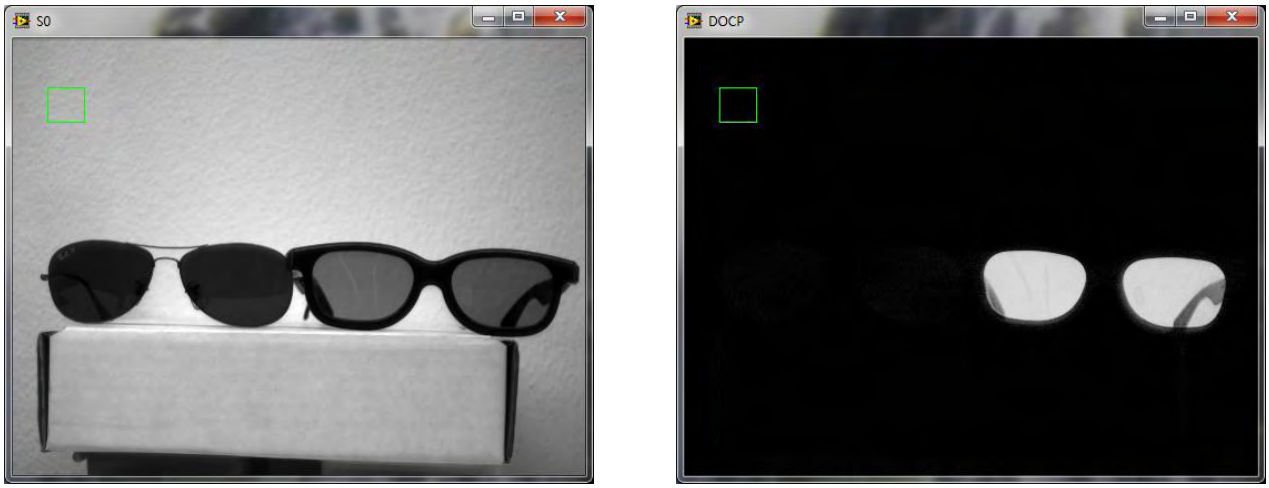

Figure 7. (a) S_0 (b) DOCP

The DOCP image shows that these 3D-movie glasses circularly polarize the light coming from the back. The background, the sunglasses on the left (which are linearly polarized) and the rest of the scene disappear in a DOCP image.

The ellipticity can be computed knowing the S_3 parameter (Figure 8).

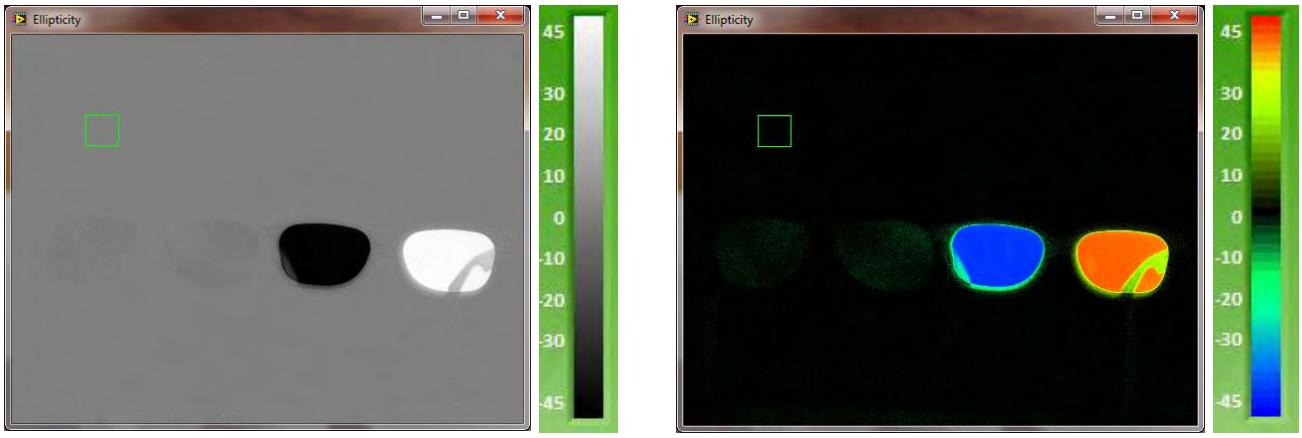

Figure 8. (a) Ellipticity (gray scale) (b) Ellipticity (false color)

With this representation the circular polarization effect can be completely analyzed. The left glass acts as a right-handed circular polarizer since the ellipticity angle is close to -45° whereas the right glass acts as a left-handed circular polarizer, with an ellipticity close to +45°.

5.4 DOP

It is also useful to visualize the Degree Of Polarization (DOP), which includes both linear and circular polarizations. Figure 9 shows the DOP image of the two pairs of glasses. They both appear bright, with no distinction of linear or circular polarization. The DOP on the sunglasses (about 60%) is lower than the one observed on the 3D-movie glasses (85%).

Figure 9. Degree Of Polarization (DOP)

6 POTENTIAL APPLICATIONS - EXAMPLE

In previous work[17], we presented many possible applications for the first version of our camera (linear Stokes polarization imaging), such as target detection/contrast enhancement[8-11], specular reflection removal, or 3D shape information extraction[20-25]. The camera presented in this publication is a full Stokes polarization imager. Additionally to the previous application presented, it is possible to integrate it as a fast PSA into a Mueller polarimeter in order to perform retardance mapping. This opens the door to stress measurement[26, 27] and various bio-medical imaging applications.

We tried to visualize polarization information on a stressed material. We took a plastic CD case and illuminated it with a linear polarization (horizontal axis). We computed all the polarization parameters with the camera, observing the CD case in transmission. Figure 10 shows the intensity S_0, the DOLP and the DOCP. It is not straightforward to interpret these images as many effects are coupled like depolarization, diattenuation and retardance. However, we can still observe a strong circular polarization signature, particularly visible close to the sides where the mechanical constraints are usually the strongest. This means birefringence effects are strong. Figure 11 shows color data fusion images, HSL (Hue, Saturation, Luminance) with Hue=AOP, Sat=255, Luminance=DOLP for the first one and Hue=ε, Sat=255, Luminance=DOCP for the second one. This allows visualizing all the polarization information (linear or circular) coded in a single image. Figure 12 shows the same CD case where we zoomed in on the bottom left corner. We can observe again that the birefringence is very strong close to the high constrained areas where both AOP and Ellipticity patterns feature fast variations. No numerical estimation of the retardation can be performed here with only a single measurement since many polarization properties are competing. Estimation of Mueller matrix and using a decomposition algorithm[5,26] would provide a numerical estimation of the retardation properties, which can be linked to mechanical stress under certain conditions and assumptions[27].

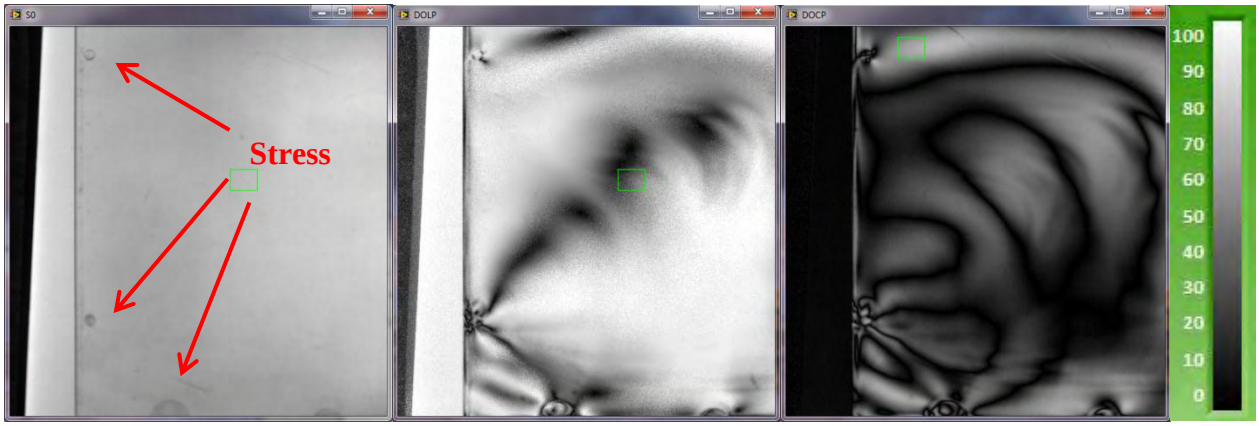

Figure 10. (a)S_0, (b)DOLP (c) DOCP

6.1

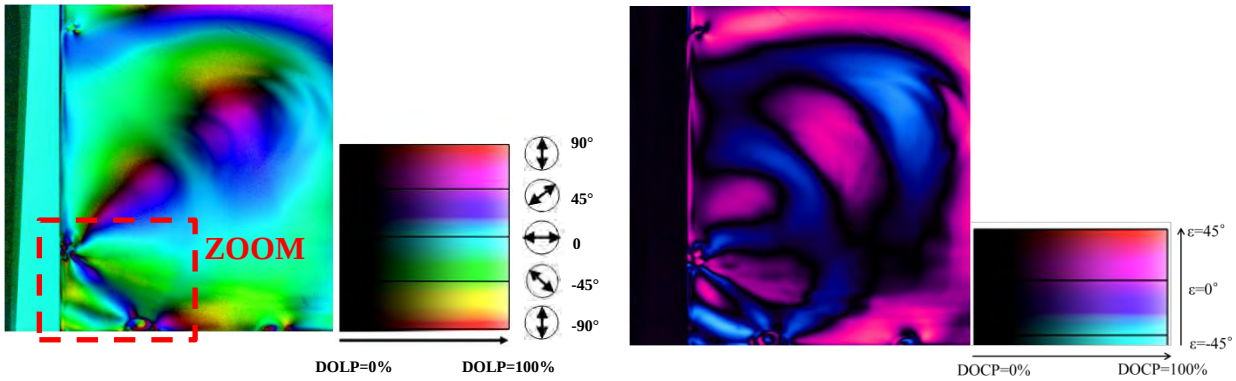

Figure 11. HSL Color data fusion (a) Hue=AOP, Sat=255, Luminance=DOLP (b) Hue=ε, Sat=255, Luminance=DOCP

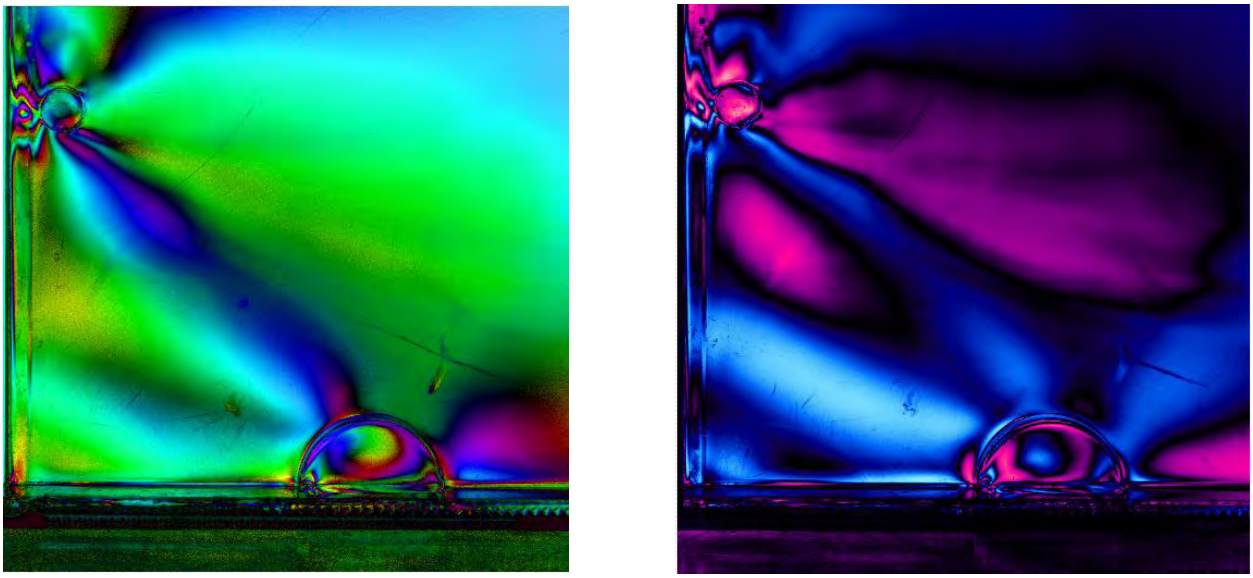

Figure 12. Zoom on the bottom-left area. (a)Fusion linear polarization (b)Fusion circular polarization

7 CONCLUSION

We have presented a full Stokes polarization camera. We focused on developing the sensor and also a powerful acquisition and processing software in order to have a live visualization and measurement of all the presented polarization parameters. This new polarization camera combines:

- Very good calibration results
- Excellent sensitivity
- Portability and robustness for field experiments
- Powerful software for live polarization measurement, analysis and visualization.
- The experimental results obtained with this camera allowed to (re)demonstrate applications of polarization imaging like:
  - target detection
  - contrast enhancement
  - reflection enhancement/removal
  - 3D reconstruction
  - Retardance mapping, stress measurement, bio-medical imaging if coupled with adequate PSG and algorithm

We will keep on improving software, acquiring more polarization data and conduct other experiments to find new applications for this versatile and user friendly sensor.

8 REFERENCES

[1] Collett Edward, [Polarized Light], M. Dekker, (1993).

[2] Goldstein Dennis L., [Polarized Light], Marcel Dekker, New York, (2003).

[3] Chipman E. A., "Polarimetry," in Hanbook of Optics, M. Bass, ed., 2, ch. 22, McGraw-Hill, New York, 2 ed., (1995).

[4] Azzam R.M.A, "Mueller matrix ellipsometry: a review", SPIE vol. 3121, August 1997, (1997).

[5] Lu Shih-Yau & Chipman Russell A., "Interpretation of Mueller matrices based on polar decomposition", J.O.S.A., Vol 13, No.5, May 1996, (1996).

[6] Collot L., Breugnot S., Larive M., "Volume perception by polarimetric imaging of the black-body radiations" , Thomson-CSF Optronique, rue Guynemer, BP 55, 78283 Guyancourt Cedex, France, Automatic Target Recognition VIII, Aerosense 98, (1998).

[7] Breugnot S., Le Hors L., Dolfi D. and Hartemann P., "Phenomenological model of paints for multispectral polarimetric imaging", AeroSense, Orlando, (2001).

[8] Goudail1 François[2], Terrier Patrick[2], Takakura Yoshitate[3], Bigué Laurent[4], Galland Frédéric[1], DeVlaminck Vincent[2], "Target detection with a liquid crystal-based passive Stokes polarimeter", [1] PhyTI group, Fresnel Institute, UMR CNRS 6133,Marseille, France; [2] MPV group, I3D,FRE CNRS 2497, Lille, France; [3] TRIO group, LSIIT, UMR CNRS 7005, Strasbourg, France; [4] MIPS, EA 2332, Mulhouse, France; submitted to Applied Optics - April 2003, (2003)

[9] Scott Tyo J., Goldstein Dennis L., Chenault David B., and Shaw Joseph A., "Review of passive imaging polarimetry for remote sensing applications", Applied Optics, Vol. 45, N22., August (2006).

[10] Larive M., Collot L., Breugnot S., Botma H., Roos P., "Laid and flush-buried mines detection using 8-12 µm polarimetric imager", Thomson-CSF Optronique, rue Guynemer, BP 55, 78283 Guyancourt Cedex, France, Aerosense 99, (1999).

[11] Clémenceau P., Breugnot S., and Collot L., "Polarization diversity active imaging", Proc. SPIE 3059, 163-173 (1997).

[12] Breugnot S., Clémenceau P., "Modeling and performances of a polarization active imager at □=806 nm", Optical Engineering, Vol.39, No. 10, 2681-2688, Oct 2000, (2000).

[13] Clémenceau P., Dogariu A., Stryjewski J., "Polarization active imaging", Thomson-CSF Optronique, Center of Research and Education in Optics and Lasers, Innovative Science and Technology Experimentation Facility, SPIE Aerosense 2000, (2000).
[14] Breugnot S., Le Hors L. and Hartemann P., "Multispectral Polarization active imager in the visible band", AeroSense, Orlando, (2000).
[15] Francia P., Bruyère F., Thiéry J.-P., Penninckx D., "Simple polarization mode dispersion compensator", Electron. Lett., vol. 35, pp 414, (1999).
[16] Dupont L., Sansoni T., de Bougrenet de la Tocnaye J. L., "Endless smectic A* liquid crystal polarization controller", Opt. Commun., vol. 209, pp 101-106, (2002).
[17] Lefaudeux N., Lechocinski N., Breugnot S., Clemenceau, P, Bossa Nova Technologies, "Compact and robust linear Stokes polarization camera", *SPIE conference*, Polarization: Measurement, Analysis, and Remote Sensing VIII, Volume 6972, 2008
[18] Gendre L., Foulonneau A., Bigué L., "Full Stokes polarimetric imaging using a single ferroelectric liquid crystal modulator", Proc. SPIE 7672, 76720B (2010)
[19] R. M. A. Azzam, I. M. Elminyawi, and A. M. El-Saba, "General analysis and optimization of the four-detector photopolarimeter," J. Opt. Soc. Am. A 5, 681–689 (1988).
[20] Atkinson Gary A., "Surface Shape and Reflectance Analysis Using Polarisation", submitted for the degree of Doctor of Philosophy ,Department of Computer Science, University of York, May 2007, (2007).
[21] Rahmann Stefan and Canterakis Nikos, "Reconstruction of Specular Surfaces using Polarization Imaging", Institute for Pattern Recognition and Image Processing, Computer Science Department, University of Freiburg, 79110 Freiburg, Germany.
[22] Morel Olivier, Meriaudeau Fabrice, Stolz Christophe, Gorria Patrick, "Polarization Imaging Applied to 3D Reconstruction of Specular Metallic Surfaces", Le2i - CNRS UMR5158, 12 rue de La Fonderie, 71200 Le Creusot, France.
[23] Morel Olivier, Meriaudeau Fabrice, Stolz Christophe, Gorria Patrick, "Active Lighting Applied to 3D Reconstruction of Specular Metallic Surfaces by Polarization Imaging", Le2i UMR CNRS 5158, 12 rue de la Fonderie, 71200 Le Creusot, France, Optical Society of America (2005).
[24] Miyazaki Daisuke, Takashima Noriyuki, Yoshida Akira, Harashima Eiki, Ikeuchi Katsushi,"Polarization-based Shape Estimation of Transparent Objects by Using Raytracing and PLZT Camera,",in Proceedings of SPIE (Polarization Science and Remote Sensing II, Part of SPIE's International Symposium on Optics and Photonics 2005), Vol. 5888, pp. 1-14, San Diego, CA USA, Aug. 2005, (2005).
[25] Vedel M., Breugnot S., Lechocinski L., "3D shape reconstruction of optical element using polarization", Proc. SPIE 7672, 767203 (2010)
[26] Richert M., Orlik X., De Martino A., "Imaging polarimetry for the determination of stress constraint in transparent solids", EPJ Web of Conferences 5, 01003 (2010)
[27] Coelho J. M. P., Silva S., Almeida T., "Stress Analysis in Glass Artwork", International Journal of Optics, Volume 2011, Article ID 215404